ELSEVIER

Colloidal films of SiO₂ in elastomeric polyacrylates by photopolymerization: A strain sensor application

Ezgi Inci, Gokhan Topcu, Mustafa M. Demir*

Department of Materials Science and Engineering, İzmir Institute of Technology, 35430, Gülbahçe, Urla, İzmir, Turkey

ABSTRACT

Thin layer SiO₂ colloidal films show angle-dependent coloration (iridescence) based on constructive interference, rather than absorption, without the existence of pigments. The transfer of thin layered colloidal film into a transparent elastomeric matrix maintaining its color may allow the fabrication of colorimetric strain sensors. In this study, trilayer SiO₂ colloidal films were prepared by Langmuir-Blodgett deposition using a binary solvent system (chloroform/methanol) and this structure is successfully transferred into poly(ethylene glycol) phenyl ether acrylate elastomer via lateral capillary force. The resulting composite films exhibit iridescence depending on the particle size, therefore, film thickness as similar in mere colloidal films with a slight difference due to change in efficient refractive index (n_{eff}). Uniaxial extension of the composite film up to 50 % strain causes a remarkable linear shift in reflection signal from 568 to 496 nm. The change in thickness of the composite film accordingly intercolloidal distance normal to the application of mechanical stretching causes variation of the reflection of light.

1. Introduction

Colorimetric sensing has become a prominent detection method in chemical diagnosis and environmental monitoring depending on external alterations in real-time [1–3]. A wide variety of colorimetric sensors has been employed on the basis of the structural change of organic dyes [4], catalysis of enzymes [5], aggregation of plasmonic nanostructures [6], etc. Among these strategies for the development of colorimetric sensing, photonic nanostructures have received considerable attention since they are able to possess vivid structural colors in the entire visible spectrum [7,8]. By integrating these structures into the polymers as color source, a series of stimuli-responsive colorimetric composites for the change in ionic strength [9,10], temperature [11], type of solvent [7,12], the concentration of biomolecules [13], and mechanical forces [14,15] have been reported. The colorimetric response upon external stimuli can be obtained from physical phenomena including interference and diffraction of the incident light [16–18]. For a variation of the color according to the magnitude of stimuli, the common strategy is based on the change of pathway of light, which governs the wavelength of resulting reflection.

To obtain colorimetric mechanical sensors, various combinations of the colloidal/polymeric materials with a number of methods have been exploited [19]. The general approach is the filling of interstitial spaces of colloidal or opal arrays with an elastomer, which results in strain responsive materials [20,21]. Sun et al. [21] reported mechanochromic fibers that are prepared by depositing polymer microspheres onto a continuous aligned-carbon-nanotube sheet and embedding into poly (dimethylsiloxane). According to the center-to-center distance of microspheres, the fibers show spectral change upon the strain. Alternatively, melt-induced assembly of nanoparticles consisting of an inelastic core and elastic shell has been developed and allows a spectral shift from 650 to 500 nm [22,23]. However, plastic deformation of the resulting films may cause the development of hysteresis and limits the reversibility since the low volume fraction of elastomers causes insufficient volume for the re-arrangement of the colloidal particles. Embedding of a non-close packed structure by swelling of the elastomer precursor can allow the reversibility. For instance, Fudouzi et al. [24,25] reported the integration of the colloidal polystyrene spheres into the silicon-based rubber and its reversible colorimetric response upon elastic deformation. Lee et al. [15] associated various fractions of the colloidal silica particles and acrylic polymer and fabricated in elastic and reversible structural colored materials. Capillary force-induced integration is considered to be the mechanism that allows the controllable and liquid-free process [26].

The reduction of the number of colloids in an elastomeric composite is the main issue for the preparation of potential sensors. The

---

* Corresponding author.
E-mail address: mdemir@iyte.edu.tr (M.M. Demir).

development of colorimetric sensors having a thin layered colloidal film with the feature of structural color may arise interest for practical applications. The preparation of photonic films using the Langmuir-Blodgett (LB) technique has been reported in numerous papers [27–29]. In general, the colloids are forced to align between air/subphase interfaces. Then, 2D monodispersed colloids are coated on substrate moving vertical or horizontal direction. This layer-by-layer fabrication allows control over the number of layers, however, it causes a lack of orientation [28]. Its control over the amount of using building blocks is a promising route to reduce the consumed colloidal particles, especially for sensor applications. One of the most important aspects distinguishing this study from other studies is the minimization of the consumption of colloids by obtaining the desired number of layers by Langmuir Blodgett deposition.

In this study, the formation of composite elastomer consisting of poly(ethylene glycol) phenyl ether acrylate (PEGPEA) and trilayer colloidal film of SiO_2 is reported. The colloidal film assembly was prepared by LB deposition. The three-layered film was integrated to a photopolymerizable acrylate monomer precursor solution and the colloidal structure was fixed by photopolymerization. The resulting composite film shows an elastic nature. As a reflection of structural change, the colorimetric variation of the composite film is examined by spectroscopy upon application of uniaxial tension.

2. Experimental

2.1. Materials

Tetraethyl orthosilicate (TEOS, 99 %), ammonia (25 % v/v aqueous solution of $NH_3 \cdot H_2O$), hexadecyltrimethylammonium bromide (CTAB), concentrated sulfuric acid (H_2SO_4, 98 %), chloroform (99 %), hydrogen peroxide (H_2O_2, 30 % v/v aqueous solution), poly(ethylene glycol) phenyl ether acrylate (PEGPEA), and 2-hydroxy-2-methylpropiophenone (97 %) were purchased from Sigma Aldrich. Ethanol (> 96 %) and 2- propanol (IPA, ≥99.5 %) were supplied from Tekkim. The deionized water (18.2 MΩ·cm^{-1} at 25 °C) used in all experiments was produced by a Milli-Q Advantage water treatment system. All chemicals were used as received without further purification.

2.2. Methods

2.2.1. Preparation of SiO_2 colloids

Monodisperse SiO_2 particles were synthesized by the modified Stöber method [30]. Firstly, the desired amount of ammonia (from 1 to 2 mL), ethanol (from 20 to 30 mL), and distilled water (from 0.5 to 1 mL) were mixed in a glass container under sonication. TEOS (1 mL) was added into the solution. The reaction was mixed until a transparent solution transform to opaque white dispersion. The mixture was then centrifuged at 6000 rpm for 30 min to sediment the colloidal particles and the precipitate was washed by ethanol three times to eliminate unreacted TEOS. Finally, the resulting white powders were dried at room temperature under 200 mbar for 24 h.

Surface modification of colloidal SiO_2 particles was carried out by employing cationic surfactant, i.e. CTAB, to obtain partially hydrophobic surfaces. Initially, an amount of bare SiO_2 particles (0.1 g) was dispersed in 5 mL of IPA under sonication for 24 h, and CTAB (4 mg) was then added into the dispersion. Subsequently, the probe sonication process was applied to achieve complete homogenization (12 min, 12 kHz, 1:2 pulse). Eventually, the dispersion was three times centrifuged and washed with IPA to remove free CTAB (6000 rpm, 30 min). Finally, CTAB modified particles were dried at room temperature for 24 h. The particles were then dispersed in a mixture of chloroform and methanol (4:1, v:v) to spread onto the water subphase. The concentration of dispersion was fixed to 10 mg/mL in all experiments.

2.2.2. Preparation of trilayer SiO_2 photonic films

Microscope glass slide (20 × 20 mm^2) was used as a substrate for trilayer deposition. First, the slides were rigorously cleaned by sonication for 10 min in acetone, ethanol, and deionized water, respectively. Then, the substrates were immersed in the mixture of H_2SO_4 and H_2O_2 (3:1, v:v) in order to activate hydroxyl groups. The resulting substrates were then dried by nitrogen.

The CTAB modified SiO_2 dispersions were homogenized in an ultrasonic bath for 30 min. LB deposition system (KSV NIMA small trough) equipped with trough, barriers, Wilhelmy plate, and horizontal robotic arm, was used to obtain colloidal film. The trough was completely filled by deionized water. The dispersions were spread on water surface by using microsyringe and volume of dispersion was kept constant (100 μL) in all depositions. After waiting 45 min, the compression process was started to form a 2D monolayer of the particles on water sub-phase. Barriers were moved with a speed of 1 mm min^{-1} until the desired surface pressure. The particles were then deposited onto the glass substrate by pulling with a speed of 1 mm·min^{-1} towards upstroke direction at constant surface pressure. The deposition process repeated three times by coating towards only upstroke direction to produce trilayer photonic films.

2.2.3. Fabrication of strain responsive films

The strain responsive elastomers were fabricated by photopolymerization of the reactive solution in the presence of photonic
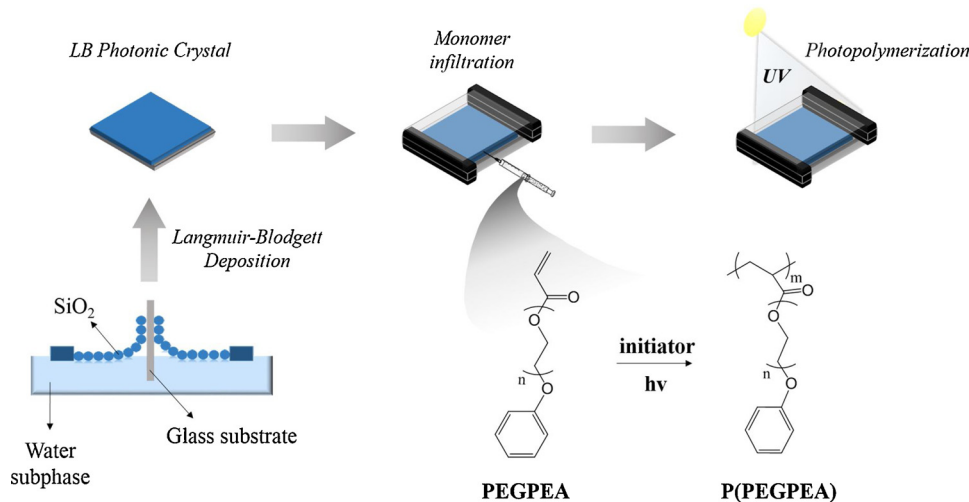
Scheme 1. Schematic illustration of the fabrication of strain responsive P(PEGPEA)/SiO_2 films.

films. The schematic illustration of the followed procedure was presented in Scheme 1. The obtained photonic films were placed to the gap between two glass slides separated by 1.0 mm thick spacers. The reactive solution was prepared by mixing PEGPEA and photoinitiator (96:4, v:v) and was rapidly injected to the gap that results in smooth spreading due to lateral capillary force. The monomer was allowed to penetrate into voids between the colloidal particles and wet their surface for 30 min. The system was irradiated by UV light at 365 nm wavelength (Osram, Vitalux, 300 W) for 3 min. The resulting polymerized composite film was carefully peeled off from the glass substrate.

2.3. Characterization

Particle size was determined using Dynamic Light Scattering (DLS; Zetasizer Nano ZS, Malvern Instruments, Worcestershire, UK). The morphology of the nanoparticles and SiO_2/P(PEGPEA) films was investigated by Scanning Electron Microscopy (SEM; Quanta 250, FEI, Hillsboro, OR, USA).The reflection spectra of the photonic films were recorded by a spectrometer (USB2000+, Ocean Optics Inc., Dunedin, FL, USA) via premium fiber cable. The photographs of the films were taken with a cell phone camera (Apple, IPhone 7, CA, USA). The regularity of the structures was determined by applying Fast Fourier Transform (FFT) to SEM images. An operational plug-in of Image J software was used to obtain 2D images in reciprocal space.

3. Results and discussion

Spherical colloidal particles of SiO_2 were obtained in the alkali medium using the Stöber method. TEOS as starting molecules undergo subsequent hydrolysis and condensation following sol-gel mechanism such that a SiO_2 network is obtained. Since the formation of the particles follows the collapse of primary nuclei particles, the size of the particles was controlled by the concentration of TEOS in the reaction. All trials are listed in Table 1. The dilution of TEOS was performed by EtOH as a solvent. Meanwhile, pH of the medium was fixed to 11 using an ammonia solution. Size distributions of the resulting SiO_2 colloids using various TEOS:EtOH ratio is presented in Fig. 1a. As the concentration of TEOS decreases from 0.22 to 0.15 M, the average particle size decreases from 280 to 175 nm. The distribution of the particles is uniform and Gaussian-type with the polydispersity index of below 0.05 for all trials.

LB deposition provides controlled compression of the monolayer of the colloids at the air-water interface for the amphiphilic materials. Since the surface of the colloids has hydrophilic nature, a surface modification for colloidal SiO_2 particles is needed [28]. The surface of the particles was treated with CTAB molecules to spread onto the water surface. The surface zeta potential of the particles increases with approximately 40 mV difference for all trials. Surface modification through CTAB enables both partially hydrophobicity and improvement of intercolloidal actions to achieve 2D monolayer onto the water surface. The colloids in the water-air interface were gathered by moving barriers. Fig. 1b shows the isotherm curves of spreading SiO_2 colloidal particles as a function of surface area. In all cases, the surface pressure of the mixture increases as the surface area decreases. Initially, the

injection of the colloids onto the water surface causes a minor increase in surface pressure since they contaminate the water surface. So that the colloids are away from each other, namely the number of colloids per unit area is relatively low. Therefore, initial surface pressure is observed minimum, i.e. gaseous-like phase. The compression via barriers reduces the distance between the colloids, which increases the surface pressure up to complete assembly. These satisfied solid-like isotherms indicate the formation of the densely packed nanostructure in a 2D array that allows the ordered transfer to the glass substrate. In addition, the dispersant (chloroform:methanol) changes the wetting ability of the particles, thereby affecting the formation of counter ion clouds around the particle. According to phase transition in the isotherms, the transfer pressure of the monolayers consisting of the colloids with a diameter of 175, 230, and 280 nm is measured 35, 24, and 30 mN/m, respectively (Table 1). The similar transfer pressure values were used for each step of the coating process to fabricate trilayer SiO_2 colloidal films. The multilayered structure was produced by moving up the substrate in a vertical direction.

SEM images of the resulting trilayer SiO_2 colloidal arrays with various particle sizes are given in Fig. 2a–c. The images suggest that the assembly of colloidal particles was successfully achieved by LB deposition. The periodicity of particles is found in a short-range. On the contrary, the long-range order lacks structure and particles exhibit a non-close packed arrangement. This level of colloidal arrangement confirms that LB provides control over the number of layers in normal direction of the film while the order of structure is relatively lower compared to conventional coating methods [28]. To quantify the effective ordering and the average distance between the particles, 2D FFT patterns of the SEM images are processed and given as insets. The concentric circles of patterns indicate that the films have short-range periodic order rather than a complete film structure. The number of circles hints about the magnitude colloid correlation in space [31]. Therefore, this periodicity correlation extends over approximately 3 particles for smaller sized spheres (175 and 230 nm) while the film contains 4 particles for the largest one (280 nm). On the other hand, the radial distribution functions of the particles were calculated from corresponding SEM images by using 16 different circles (r: 3.5 μm). The representative circle and corresponding plots of the resulting functions are presented in Fig. 2d and e, respectively. The intensity of the signals decreases as the radius increases, which also suggests the short-range order of the colloidal array. Therefore, it can be concluded that the resulting trilayer films have short-range ordered and non-close packed structures. Note that the degree of order is equal or larger than three particles, hence, the three layers of colloidal arrays may vertically persist their periodicity.

For topological examination, AFM was employed to determine the surface periodicity of the SiO_2 colloidal films. Topography and 3D images of the structure consisting of SiO_2 colloidal particles (230 nm) are presented in Fig. 2f. The top layer of the colloidal film presents local hexagonal and periodic domains. In addition, the 3D image gives information regarding the roughness of the structure. The height difference between the particles in the topmost layer falls approximately to 100 nm to the bottom layer. This height difference is less than particle size. Therefore, the degree of roughness also hints about the formation of a non-close packed structure.

The reflection spectra and as well as the photographic images of the resulting trilayer structures are given in Fig. 3. The angle of reflected light causes a dramatic shift in the reflection spectrum for all three structures. The maxima of reflection wavelength (λ_{max}) decrease as the incident angle increases. In general, Bragg-Snell's law expresses the change in reflection wavelength of periodic micro- or nanostructures;

$$\lambda_{max} = 2d_{(111)}\sqrt{(n_{eff}^2 - sin^2\theta)} \tag{1}$$

where the lattice spacing of the (111) plane is $d_{(111)}$, the effective refractive index is n_{eff}, and the incident angle of reflected light is θ. The
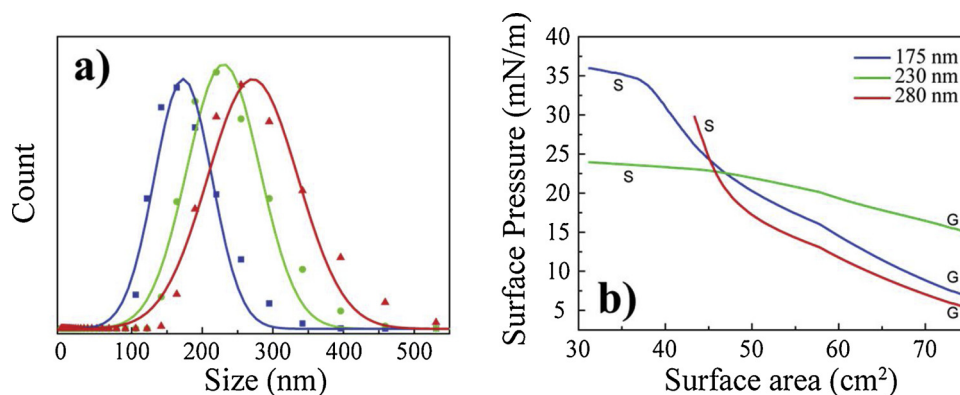
Table 1
Features of SiO_2 colloidal particles and synthesis conditions.

Samples	ratio (v:v)		D (nm)	PDI	ζ potential (mV)		Surface Pressure (mN/m)
	EtOH	TEOS			Bare	Modified[a]	
1	30	1	175	0.024	−59	−3,56	35
2	25	1	230	0.048	−35	20,6	24
3	20	1	280	0.019	−7,31	22,4	30

[a] By CTAB of 4.0 mg.

Fig. 1. (a) DLS size distribution of the SiO$_2$ colloidal particles, (b) μ-A isotherms of the spreading particles for trilayer fabrication.
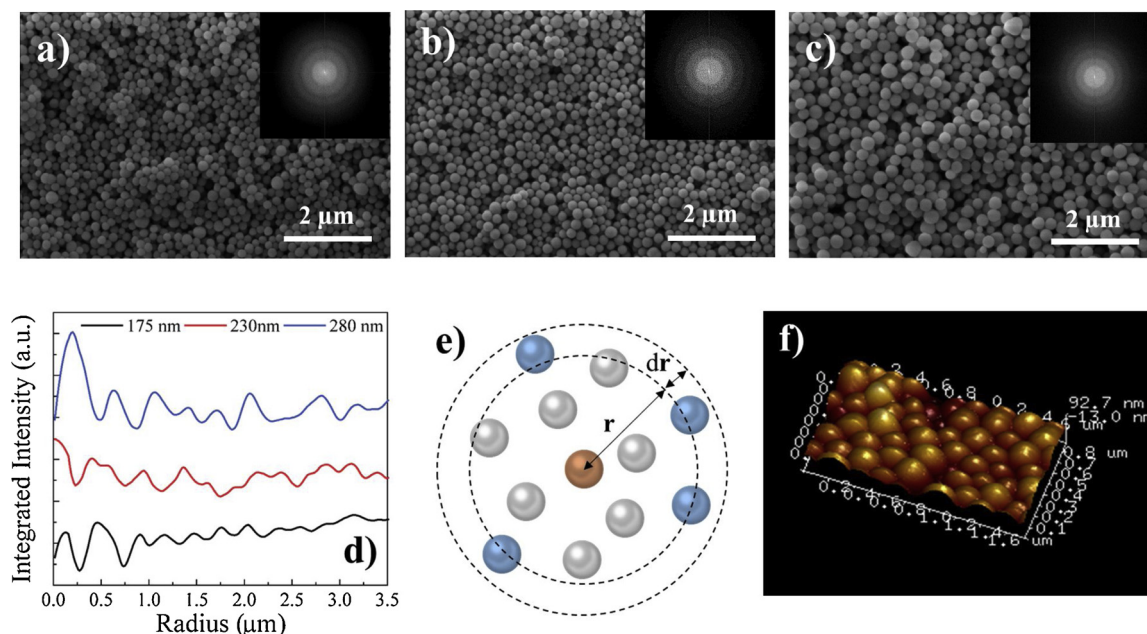

Fig. 2. (a–c) SEM images of trilayer films having different particle size with corresponding FFT images (inset). (d) Calculated radial distribution functions of colloidal arrays and (e) its schematic representation. (f) 3D AFM images of trilayer film with particle size of 230 nm.

$d_{(111)}$ can be calculated by using the diameter of the particle (D) for the HCP structure.

$$d_{(111)} = \left(\frac{\sqrt{3}}{2} \right) D \tag{2}$$

Since the colloidal array consists of the particles and air gaps, n_{eff} is considered as a basis of refractive indices (n_s: 1.45 and n_{air}: 1.00 at 632 nm) and volume fractions (f) and can be calculated as follows:

$$n_{eff} = (n_s{}^2 f_s + n_{air}{}^2 (1 - f_s))^{1/2} \tag{3}$$

Theoretically, λ_{max} through changing incident angle shifts from 400 to 265 nm when the diameter is 175 nm. Similarly, the wavelength changes from 530 to 350 nm and from 625 to 415 nm for the particle diameters of 230 and 280 nm, respectively. According to the corresponding reflection spectra, a similar spectral shift depending on the increasing incident angle is observed with an approximate wavelength difference of 40 nm. For instance, the shift in the reflection of the particles with a diameter of 175 nm is from 430 to 370 nm as the incident angle increases (Fig. 3a). For the particle size of 230 and 280 nm, this blue-shift in the reflection spectra is observed from 490 to 420 nm and from 645 to 575 nm, respectively (Fig. 3b and c). The recorded λ_{max} is higher than the theoretical one. The difference between theoretical

and experimental reflection values may arise from the packing density of the photonic films. The calculation using Bragg-Snell's law is carried out with an assumption of close-packing that refers to 0.74 as an fs. Nevertheless, the packing density of the resulting photonic films seems lower due to a non-close packed structure. Note that the average interplanar distance in non-close packed structure would be greater than HCP. The reflection is not only detected by spectroscopy but also via eye perception (Fig. 3d and e). Bluish, green, and yellow colors are observed as the particle diameter changes. On the other hand, the distinct iridescence from violet to green (d: 230 nm) can be also observed by changing incident angle.

The colloidal film wet by prepolymer solution was exposed to UV light for photopolymerization, and the composite film of SiO$_2$ colloidal assembly was prepared in P(PEGPEA) matrix. The colloidal assembly was successfully fixed in the matrix as a result of polymerization. A representative SEM image of the surface of corresponding composites is presented in Fig. 4a–c. The periodic array of each film is transferred into the polymer matrix without any distortion in the structure. A thin curtain refers to a thin layer of polymeric film on colloidal films. The cross-section of the elastomeric composite reveals that all gaps among the colloidal particles are completely filled by P(PEGPEA) (Fig. 4d). On the other hand, the average thickness of the colloidal layer observed in the cross-sectional area is approximately three times the particle
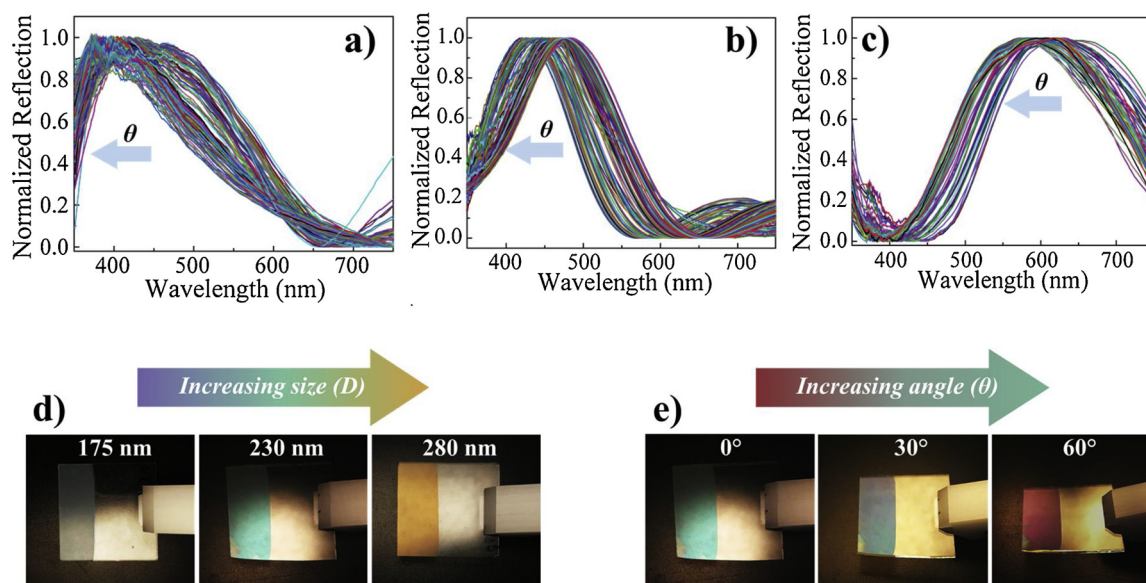
Fig. 3. (a–c) Normalized reflection spectra of trilayer films consisting of different-sized particles, photographs of their changing iridescent colors by (d) particle size and (e) incident angle.

diameter, which suggests the existence of a trilayer colloidal assembly.

Similar to naked trilayer colloidal films, the composite film exhibits distinct reflective colors (Fig. 5a); iridescent green and blue colors. The uncoated part of the film is transparent so that it enables to distinguish the colloidal array via eye perception. The low refractive index difference between bulk SiO_2 (n_s: 1.450 at 632 nm) and P(PEGPEA) (n_p: 1.505 at 632 nm) still allows scattering out of the incident light from stopband, generating an iridescent film. The optical properties of the film may also be confirmed by reflectance. In Fig. 5b, normalized reflection spectra of the film are presented. The reflection signal shifts from 554 to 480 nm as the incident angle increases. The variation in the reflection suggests the presence of at least a short-range ordered structure according to Bragg-Snell's law. Furthermore, the wavelength difference between a bare colloidal array and polymeric one is 64 nm while is θ is 0°. The difference arises from the replacement of air gaps by P(PEGPEA), which dramatically increases n_{eff}.

The colorimetric response of the material upon stretching depends on both the size of the SiO_2 colloids (due to changing Bragg Peak and interplanar distance) and the refractive index difference between the elastomer matrix and the colloids. The optical response of the film upon

mechanical stimuli was examined. The corresponding reflectance in various strains (ε_x) was recorded. The original length of the colloidal film L_0 was stretched to L by lateral tensile deformation and reflection of the film was registered for each ε_x. The reflection signal continuously shifts to lower wavelengths as ε_x increases (Fig. 6a). The peak position reaches from 569 to 496 nm when the ε_x is 0.50. The stretching normally results in a reduction in the thickness of the film, hence the decrease of interplanar distance (Fig. 6b). According to Bragg-Snell's Law, λ_{max} is indirectly governed by the strain along the lateral direction. Therefore, the strain-induced reduction in $d_{(111)}$ leads to a blue shift in the reflection spectrum. Since the elastomer composite contains only trace amount of colloidal SiO_2 particles, the mechanical behavior of composite would be similar to bare and bulk P(PEGPEA). Therefore, the change in λ_{max} by stretching may hint about Poisson's ratio of the material due to the proportional relation between interplanar distance and reflection. In Fig. 6c, the decrease in maxima is presented as a function of strain. The decreasing regime ($\Delta\lambda_{max}/\Delta\varepsilon_x$) can be found as 0.73. The change in both interplanar distance and thickness of the film with respect to ε_x is given in Fig. 6d. Not surprisingly, Poisson's ratio of the film ($-\Delta T/\Delta L$) is calculated 0.79 that is close to decreasing regime in reflection upon strain. *The International Commission on Illumination* (CIE)
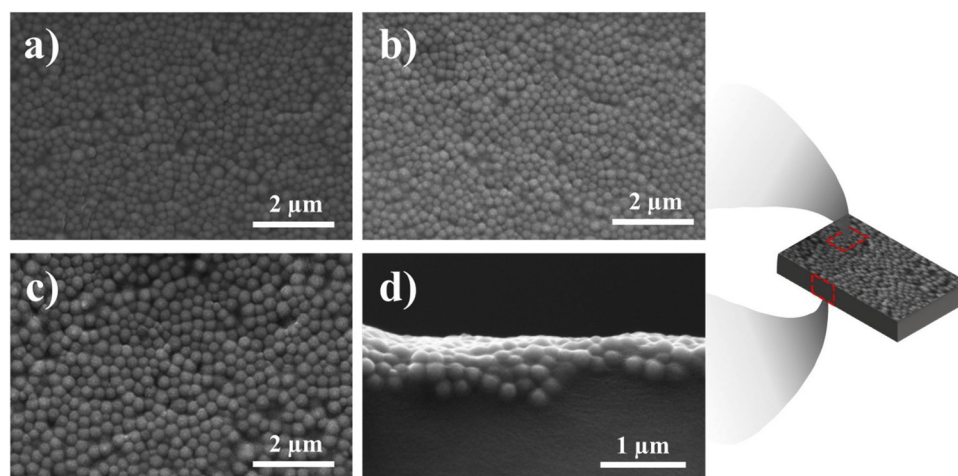
Fig. 4. (a–c) SEM images of the elastomeric P(PEGPEA)/SiO_2 composite films consisting of different-sized colloidal particles and (d) cross-section image of the film including particles with a diameter of 230 nm on the surface.
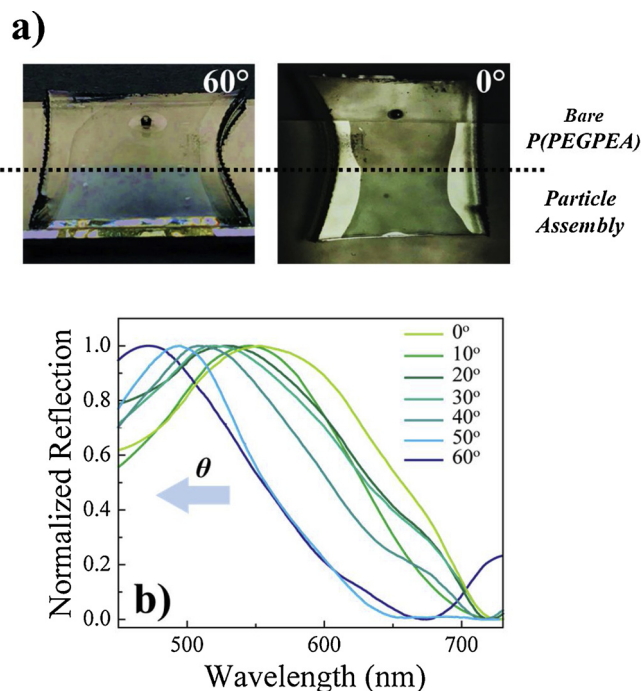
Fig. 5. (a) Photographs and (b) normalized reflection spectra of the elastomer P(PEGPEA)/SiO$_2$ composite film with the particle size of 230 nm at various angles.

1931 chromaticity diagram for strained films is presented in Fig. 6e. As the ε_x increases, the generated color gradually shifts from green to blue. Note that the coordinates are close to the center of the diagram, which indicates the intensity of the colors, is weak. The pale color is resulted through low refractive index difference (Δn) that hinders the number of scattering events. The Δn of the composite is found as 0.055 (n_p-n_s), which is lower than the photonic film having only colloidal particles (n_s-n_{air} = 0.45). Therefore, the color of the film would be relatively pale

in the presence of P(PEGPEA). On the other hand, it is observed that the strain-induced change in reflection is reversible process and optical response is fully recovered by removing the external force (Fig. 7a). Since the particles are entirely fixed in the rubber-like matrix, they are unable to change the location in three-dimensional space. Therefore, stable position of the particles leads to the complete recovery of residual strain. Further reversibility of the optical properties was examined by stretching-releasing cycles. The reflection peak position remains unchanged even after 40 % strained for three times (Fig. 7b). No hysteresis was observed for the composite samples at least for this limited number of cycling.

4. Conclusions

Monodisperse colloidal particles of SiO$_2$ were synthesized using the Stöber method. The particles were arranged onto a glass substrate as a trilayer film by using LB deposition via the binary solvent system. The resulting colloidal film exhibits iridescent saturated structural color depending on the size of constituent particles and incident angle. The trilayer deposits were wet by acrylate monomer using lateral capillary force. The key point of the process is the injection of the monomer into the film without disturbance of the compact structure. The reactive solution of PEGPEA was injected into the gap between two parallel surfaces in the presence of colloidal film. By photopolymerization, the colloidal assembly was fixed on the top layer of the elastomeric matrix and the resulting composite showed iridescence using only a minute amount of colloidal particles. Moreover, a clear spectral shift is observed when uniaxial tension is applied to the composite. Since the colloidal assembly is placed merely on the surface of the elastomeric film, LB deposition allows obtaining colorful composite films. This strategy offers a general promising way for the association of soft elastomeric matrix and colloidal LB films. The strain-responsive color-changing elastomers consisting of colloidal films of various types can be fabricated by employing this process. Compared to other strain sensors, the produced colorimetric strain sensors provide reflection control at various angles without complex data collection or display systems. Moreover, they show a colorimetric signal containing a minute amount
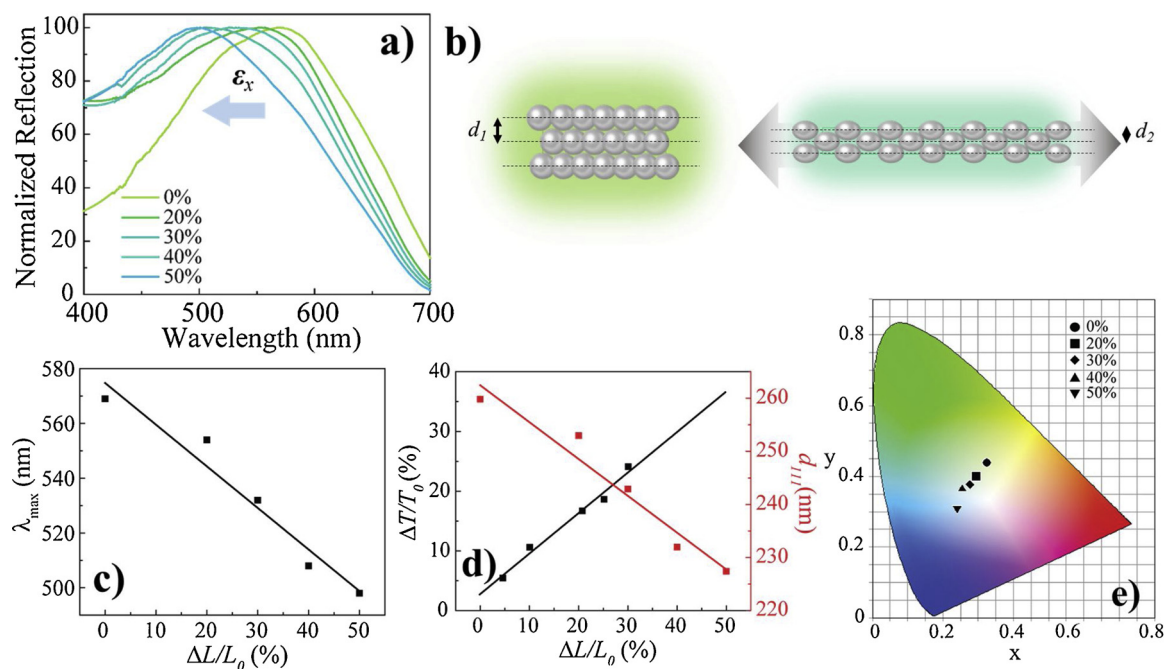

Fig. 6. (a) Reflection spectra of the composite film having particle size of 230 nm upon lateral strain, (b) schematic representation of the strain-induced structure change of particle assembly in the elastomer. Change in (c) reflection signal, (d) thickness, and $d_{(111)}$ as a function of applied lateral strain. (e) CIE coordinates of the corresponding film in various levels of extensions.
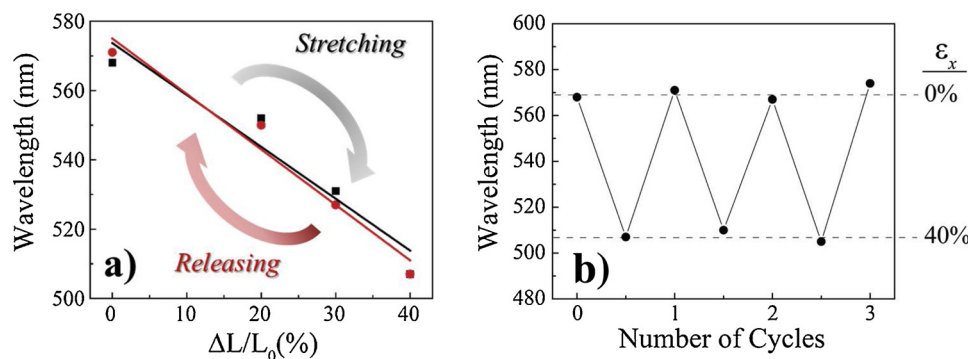
Fig. 7. Reversible optical characteristics of the films; (a) change in reflection upon gradual stretching-releasing. (b) The reflection signals as a function of cycles between lateral strains of.0–40 %.

of inorganic material. Therefore, they can be used in various applications such as display, security and camouflages based on these properties.

Authors contribution

The first two authors of the manuscript contribute equally to this study.

Declaration of Competing Interest

The authors declare that they have no known competing financial interests or personal relationships that could have appeared to influence the work reported in this paper.

Acknowledgements

Appendix A. Supplementary data

Supplementary material related to this article can be found, in the online version, at doi:https://doi.org/10.1016/j.snb.2019.127452.

References

[1] M. Saleem, M. Rafiq, M. Hanif, Organic material based fluorescent sensor for Hg 2+ : a brief review on recent development, J. Fluoresc. 27 (2017) 31–58.

[2] K.S. Suslick, N.A. Rakow, A. Sen, Colorimetric sensor arrays for molecular re-cognition, Tetrahedron 60 (2004) 11133–11138.

[3] M. Li, S.K. Cushing, N. Wu, Plasmon-enhanced optical sensors: a review, Analyst 140 (2015) 386–406.

[4] H. Sun, L. Yu, H. Chen, J. Xiang, X. Zhang, Y. Shi, Q. Yang, A. Guan, Q. Li, Y. Tang, A colorimetric lead (II) ions sensor based on selective recognition of G-quadruplexes by a clip-like cyanine dye, Talanta 136 (2015) 210–214.

[5] Y. Wang, Y. Zhu, A. Binyam, M. Liu, Y. Wu, F. Li, Discovering the enzyme mimetic activity of metal-organic framework (MOF) for label-free and colorimetric sensing of biomolecules, Biosens. Bioelectron. 86 (2016) 432–438.

[6] G. Topcu, T. Guner, E. Inci, M.M. Demir, Colorimetric and plasmonic pressure sensors based on polyacrylamide/Au nanoparticles, Sens. Actuators A Phys. 295 (2019) 503–511.

[7] H. Fudouzi, Y. Xia, Colloidal crystals with tunable colors and their use as photonic papers, Langmuir 19 (2003) 9653–9660.

[8] Y. Iwayama, J. Yamanaka, Y. Takiguchi, M. Takasaka, K. Ito, T. Shinohara, T. Sawada, M. Yonese, Optically tunable gelled photonic crystal covering almost the entire visible light wavelength region, Langmuir 19 (2003) 977–980.

[9] V.L. Alexeev, A.C. Sharma, A.V. Goponenko, S. Das, I.K. Lednev, C.S. Wilcox, D.N. Finegold, S.A. Asher, High ionic strength glucose-sensing photonic crystal, Anal. Chem. 75 (2003) 2316–2323.

[10] C. Fenzl, S. Wilhelm, T. Hirsch, O.S. Wolfbeis, Optical sensing of the ionic strength using photonic crystals in a hydrogel matrix, ACS Appl. Mater. Interface 5 (2012) 173–178.

[11] J.D. Debord, L.A. Lyon, Thermoresponsive photonic crystals, J. Phys. Chem. B 104 (2000) 6327–6331.

[12] K. Higashiguchi, M. Inoue, T. Oda, K. Matsuda, Solvent-responsive structural co-lored balloons, Langmuir 28 (2012) 5432–5437.

[13] Z. Cai, N.L. Smith, J.-T. Zhang, S.A. Asher, Two-dimensional photonic crystal chemical and biomolecular sensors, Anal. Chem. 87 (2015) 5013–5025.

[14] P. Snapp, P. Kang, J. Leem, S. Nam, Colloidal photonic crystal strain sensor in-tegrated with deformable graphene phototransducer, Adv. Funct. Mater. (2019) 1902216.

[15] G.H. Lee, T.M. Choi, B. Kim, S.H. Han, J.M. Lee, S.-H. Kim, Chameleon-inspired mechanochromic photonic films composed of non-close-packed colloidal arrays, ACS Nano 11 (2017) 11350–11357.

[16] Y. Takeoka, Stimuli-responsive opals: colloidal crystals and colloidal amorphous arrays for use in functional structurally colored materials, J. Mater. Chem. C 1 (2013) 6059–6074.

[17] Y.Y. Diao, X.Y. Liu, G.W. Toh, L. Shi, J. Zi, Multiple structural coloring of silk-fi-broin photonic crystals and humidity-responsive color sensing, Adv. Funct. Mater. 23 (2013) 5373–5380.

[18] Q. Zhao, C.E. Finlayson, D.R. Snoswell, A. Haines, C. Schäfer, P. Spahn, G.P. Hellmann, A.V. Petukhov, L. Herrmann, P. Burdet, Large-scale ordering of nanoparticles using viscoelastic shear processing, Nat. Commun. 7 (2016) 11661.

[19] J. Ge, Y. Yin, Responsive photonic crystals, Angew. Chemie Int. Ed. 50 (2011) 1492–1522.

[20] A.C. Arsenault, T.J. Clark, G. von Freymann, L. Cademartiri, R. Sapienza, J. Bertolotti, E. Vekris, S. Wong, V. Kitaev, I. Manners, From colour fingerprinting to the control of photoluminescence in elastic photonic crystals, Nat. Mater. 5 (2006) 179.

[21] X. Sun, J. Zhang, X. Lu, X. Fang, H. Peng, Mechanochromic photonic-crystal fibers based on continuous sheets of aligned carbon nanotubes, Angew. Chemie Int. Ed. 54 (2015) 3630–3634.

[22] B. Viel, T. Ruhl, G.P. Hellmann, Reversible deformation of opal elastomers, Chem. Mater. 19 (2007) 5673–5679.

[23] C.G. Schäfer, B. Viel, G.P. Hellmann, M. Rehahn, M. Gallei, Thermo-cross-linked elastomeric opal films, ACS Appl. Mater. Interface 5 (2013) 10623–10632.

[24] H. Fudouzi, T. Sawada, Photonic rubber sheets with tunable color by elastic de-formation, Langmuir 22 (2006) 1365–1368.

[25] H. Fudouzi, T. Sawada, Tuning stop band of soft opal film by deformation for strain sensing applications, Photonic Crystals and Metamaterials for Sensing Applications II, International Society for Optics and Photonics, 2006 p 63690D.

[26] D. Yang, S. Ye, J. Ge, Solvent wrapped metastable colloidal crystals: highly mutable colloidal assemblies sensitive to weak external disturbance, J. Am. Chem. Soc. 135 (2013) 18370–18376.

[27] M. Szekeres, O. Kamalin, R.A. Schoonheydt, K. Wostyn, K. Clays, A. Persoons, I. Dékány, Ordering and optical properties of monolayers and multilayers of silica spheres deposited by the Langmuir–Blodgett method, J. Mater. Chem. 12 (2002) 3268–3274.

[28] M. Bardosova, M.E. Pemble, I.M. Povey, R.H. Tredgold, The Langmuir-Blodgett approach to making colloidal photonic crystals from silica spheres, Adv. Mater. 22 (2010) 3104–3124.

[29] M. Parchine, J. McGrath, M. Bardosova, M.E. Pemble, Large area 2D and 3D col-loidal photonic crystals fabricated by a roll-to-roll Langmuir–Blodgett method, Langmuir 32 (2016) 5862–5869.

[30] W. Stöber, A. Fink, E. Bohn, Controlled growth of monodisperse silica spheres in the micron size range, J. Colloid Interface Sci. 26 (1968) 62–69.

[31] S.G. Romanov, S. Orlov, D. Ploss, C.K. Weiss, N. Vogel, U. Peschel, Engineered disorder and light propagation in a planar photonic glass, Sci. Rep. 6 (2016) 27264.

Ezgi Inci received her BSc in Material Science and Engineering (2017) from the Anadolu University and MSc in Materials Science and Engineering (2019) in İzmir Institute of Technology, respectively. She has been carrying out her PhD on inorganic nanomaterials and polymeric composites at Department of Materials Science and Engineering in İzmir Institute of Technology since September 2019. Her current researches are on the fabri-cation of Langmuir Blodgett coatings and mechanical sensors.

Gokhan Topcu received his BSc in Chemistry (2013) and MSc in Organic Chemistry (2015) from the Marmara University, respectively. He carried out his doctoral research on advanced polymeric composites and nanomaterials and received his PhD from Department of Materials Science and Engineering in İzmir Institute of Technology (2019). His current researches are on the development of mechanical sensors by using plasmonic and photonic nanostructures in polymeric systems.

Mustafa M. Demir is Professor at the Izmir Institute of Technology, Department of Materials Science and Engineering. He coordinates an interdisciplinary group working on synthesis and nanotechnologies on soft matter. His research activity is focused on the development of polymeric optical nanocomposites for advanced applications, electrospinning, and functional systems. He has been awarded the "Young researcher" Prize of Turkish Academy of Sciences in 2013. His details can be found at: http://www.demirlab.iyte.edu.tr